EARTH SCIENCES
RESEARCH JOURNAL

Earth Sci. Res. J. Vol. 21, No. 4 (December, 2017): 175-181

UNIVERSIDAD NACIONAL DE COLOMBIA

APPLIED GEOPHYSICS

Interpretation of aeromagnetic data using GIS to evaluate the geotectonic regime of the Sabinas Basin

José A. Batista Rodríguez, Yuri Almaguer Carmenates, Josue D. Martínez González
Universidad Autónoma de Coahuila. México
josebatista@uadec.edu.mx

ABSTRACT

The study present the use of Geographic Information System (GIS) to assess the geotectonic regimen of the Sabinas Basin. Initially, the GIS database was designed using geological and geophysical information (total magnetic field reduced to the pole). Subsequently, 2D models of the basin were obtained along 4 profiles running on a north-south direction. The implementation of GIS enables a geological-geophysical interpretation generating various thematic maps that overlap the magnetic map during interpretation. The analysis of overlapping maps enables the identification of areas with different geotectonic regimes in the Sabinas Basin, as well as the relationship between these environments and mineralization. The qualitative and quantitative interpretation of the aeromagnetic data obtained for the total magnetic field reduced to the pole delineate uplifted basement areas as well as shallower blocks within them. This paper presents the location of both the basin´s deepest zones and its probable faults, which can be linked to the block boundaries. The faults zones and block boundaries correspond to the main mineral deposits found in the basin. Finally, the geotectonic regime of some sectors of the basin is detailed in order to reaffirm the results obtained by the interpretation of aeromagnetic data.

Keywords: Geotectonic regime; GIS; aeromagnetic data; northeastern Mexico; Sabinas Basin.

Interpretación de datos aeromagnéticos usando SIG para evaluar el regimen geotectónico de la Cuenca de Sabinas

RESUMEN

Se presenta el uso de un Sistemas de Información Geográfica para evaluar el régimen geotectónico de la Cuenca de Sabinas. Inicialmente se llevó a cabo el diseño de la base de datos del Sistema de Información Geográfica, teniendo en cuenta las características de la información geológica y geofísica (campo magnético total reducido al polo). Posteriormente se obtienen modelos 2D de la cuenca a lo largo de 4 perfiles con direcciones norte-sur. A partir de la implementación del Sistema de Información Geográfica, se logró una interpretación geológica-geofísica, generando diversos mapas temáticos que se superpusieron al mapa magnético durante dicha interpretación. El análisis de los mapas superpuestos permitió identificar áreas con diferente régimen geotectónico dentro de la Cuenca de Sabinas, así como la relación de esas áreas con mineralizaciones. A partir de la interpretación cualitativa y cuantitativa de los datos del campo magnético total reducido al polo se delimitan áreas levantadas del basamento de la cuenca y los bloques más someros dentro de las mismas. También se localizan las zonas más profundas de la cuenca y probables fallas, que pueden estar vinculadas con los límites de los bloques. Las zonas de fallas y los límites de bloques están relacionados con los principales depósitos minerales de la cuenca. Por último, se detalla el régimen geotectónico de algunos sectores de la cuenca, para reafirmar los resultados de la interpretación de los datos aeromagnéticos.

Palabras clave: Régimen geotectónico; SIG; datos aeromagnéticos; noreste de México; Cuenca de Sabinas.

Record
Manuscript received: 08/06/2016
Accepted for publication: 23/08/2017

How to cite item:
Batista, J. A., Almaguer, Y., & Martínez J. D. (2017). Interpretation of aeromagnetic data using GIS to evaluate the geotectonic regime of the Sabinas Basin. *Earth Sciences Research Journal, 21(4).* 175-181.
Doi: http://dx.doi.org/10.15446/esrj.v21n4.57924

1. Introduction

The efficient interpretation of geophysical data requires the knowledge and appropriate use of geological information, especially information represented on geological maps. Magnetometry is a geophysical method usually used in regional geological studies. The surface and subterranean distribution of different rocks types and geological structures provide the basis for the behavior of magnetic field (Telford et al., 1990).

In sedimentary basins, the magnetic field is principally related to the crystalline basement, which is generally composed of igneous and metamorphic rocks which have a very high magnetic effect (Vázquez et al., 1990; Gunn, 1997). Deformations in the sedimentary infill of the basin may be related to their basement dynamics, which are linked to faults that cause uplifted or depressed blocks (Gunn, 1997).

The magnetic method has been used for the mineral exploration in the Sabinas Basin, which is located in northeastern Mexico (Figure 1) (Pascacio-Toledo, 2001). The deposits of metallic and nonmetallic minerals found in this basin, comprise mainly coal, fluorite, celestine, Pb-Zn-Ag and hydrocarbons (Eguiluz de Antuñano, 2001; Corona-Esquivel et al., 2006; González-Sánchez et al., 2007, 2015).

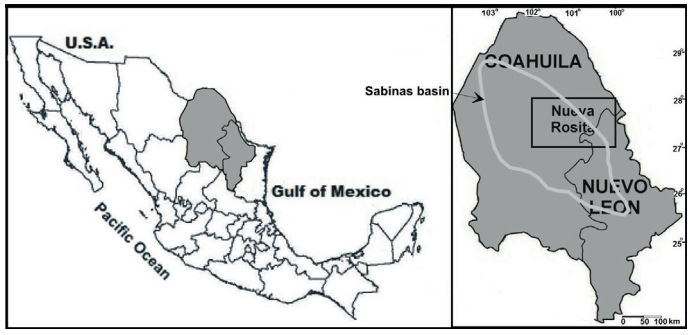

Figure 1. Location of the study area (a section of the geological map of Nueva Rosita). Light gray line indicates the border with the Sabinas Basin. Modified from Martínez-Rodríguez et al. (2008).

In the interpretation of magnetic data, it is very important to have the geological maps to identify the distribution of igneous rocks, geological structures and mineralized areas which can be linked to positive anomalies in the magnetic field. These geological maps also show the surface distribution of rocks that can be classified as diamagnetic, paramagnetic or ferromagnetic, according to their magnetic susceptibility values. Once those geological characteristics are known, they can be the behavior of the magnetic fields. GIS techniques are widely used to integrate geological and geophysical data, because they provide effective tools for managing geo-referenced information by enabling the correlation and comparison of different types of information. The graphical, numerical and text information can be combined using these tools (Ziaii et al., 2010; Khemiri et al., 2013). For example, in this study, fault locations (graphical information) with their respective names (text information), with values of magnetic anomalies (numerical data) can be combined, generating several maps of interpretation.

This research presents an example of using GIS, combined with other tools, to use maps to interpret geophysical data, taking as an example, the aeromagnetic data reduced to pole obtained for the Nueva Rosita area, in order to assess the geotectonic regime in this section of the Sabinas Basin, located in northeastern Mexico (Figure 1).

2. Geological setting

The study region is located in the Sabinas Basin in northeastern Mexico (Figure 1). This basin forms part of a rift associated with the opening of the Gulf of Mexico (Eguiluz de Antuñano, 2001). This structure originated as a rift-type graben limited by paleotectonic and paleogeographic blocks, such as the Coahuila block to the southwest (SW), the Tamaulipas block to the northeast (NE), and the Burro-Peyotes blocks to the north (N) (Figure 2). The San Marcos and La Babia faults are deep regional structures that separate the blocks of the basin (Chávez-Cabello et al., 2005).

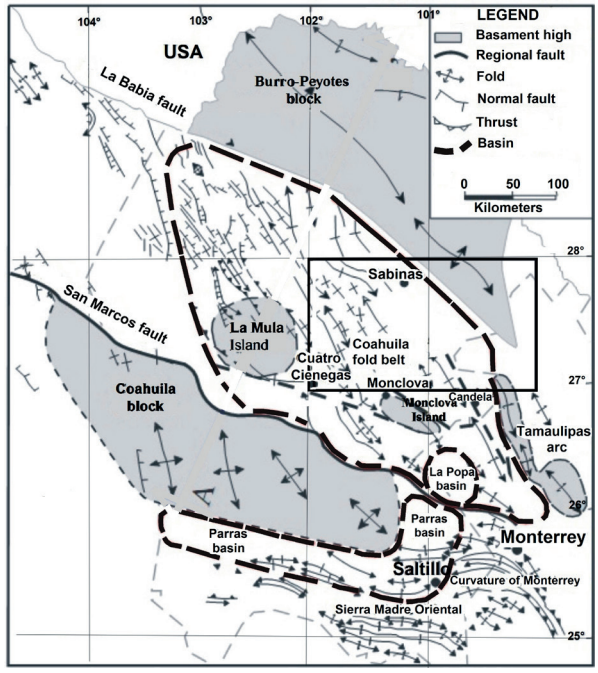

Figure 2. Structural configuration and tectonic features of northeastern Mexico (Coahuila and adjacent areas). Rectangle indicates the study area. Taken from Chávez-Cabello et al. (2005).

The Sabinas Basin is filled with different types of sedimentary rock, principally limestone, sandstone, shale, conglomerate, limolite and gypsum, accumulated during the Mesozoic and Cenozoic (Eguiluz de Antuñano, 2001; González-Sánchez et al., 2007). In the Late Cretaceous, the Laramide orogeny altered the sedimentary regime in the region and caused deformation in all sedimentary sequences (Eguiluz de Antuñano, 2001). This orogeny was also accompanied by various magmatic events which generated different types of igneous rocks during the Middle Eocene (basic, intermediate and acidic rocks), constituting some intrusive bodies that outcrop in the Candela-Monclova intrusive belt located to the southeast of the Sabinas Basin (Chávez-Cabello et al., 2011).

The geological map of Nueva Rosita (Martínez-Rodríguez et al., 2008) is located in the Sabinas Basin (Figure 2 and 3). Outcroppings of sedimentary rocks are found in the entire area covered by the map, aside from the central-north part of the map, named Esperanzas-Kakanapo lava , in which volcanic rocks outcrop (Martínez-Rodríguez et al., 2008). Various anticline and syncline folds are observed in this region, whose axes lie northwest-southeast (NW-SE). Also there are also several fault systems following the same direction. Some of the identified anticline folds being heavily eroded, such as the Obayos anticline (Figure 3). A high level of erosion in this structure causes outcropping in the majority of the sedimentary Mesozoic sequence (Martínez-Rodríguez et al., 2008). Metallic and nonmetallic mineral deposits can also be found in this area (Figure 3). The nonmetallic mineralization mainly comprises coal (Corona-Esquivel et al., 2006), barite, celestine, fluorite and hydrocarbons, whereas Ag-Pb-Zn comprises the most significant metallic mineralization (González-Sánchez et al., 2007, 2015). The deposits of barite, celestine, fluorite and Ag-Pb-Zn are Mississippi Valley-Type (MVT) mineral deposits (González-Sánchez et al., 2007).

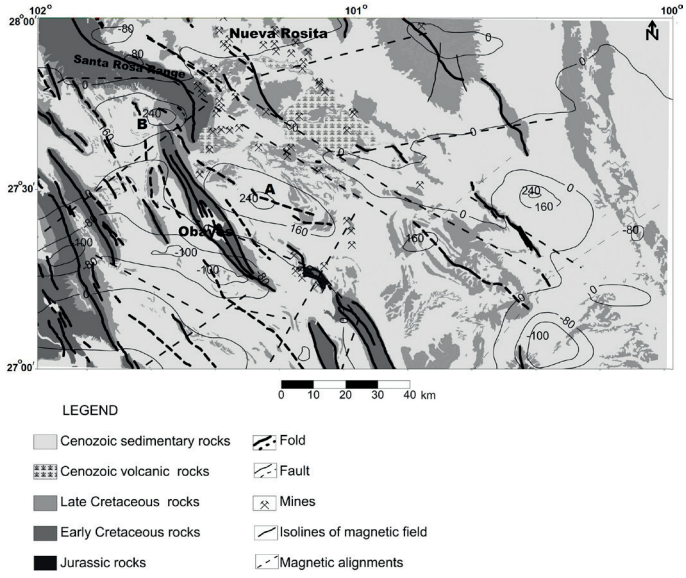

Figure 3. Simplified geochronological map of Nueva Rosita (modified from Martínez-Rodríguez et al., 2008). The black symbol indicates the location of mineral deposits of coal, barite, celestine and fluorite. The letters A and B indicate the uplifted blocks of the basement that correspond to surface deformations.

3. Methodology

The GIS database structure was designed to include geological and geophysical information from previous research undertaken by Martínez-Rodríguez et al. (2008) and SGM (2000), as well as, results of the interpretation of geophysical data. The structure of the database included the objects considered (geological information, tectonic, aeromagnetic data, etc.), as well as the type of object (areal, vector or point) its attributes (name, rock types, mineralization, values of the magnetic field, etc.) and type of field (integer, logical and character). Subsequently, the input of geological and geophysical data was performed under the categories of object type, attribute and field type. The representation and management of all the information was made the geographical coordinates system. The geological and geophysical interpretation was carried out in the final stage of GIS management, overlapping and comparing the set of geological and geophysical information used. The geological information is based on the geological map of Nueva Rosita to a scale of 1:250, 000 (Martínez-Rodríguez et al., 2008). This geological map provided information pertaining to outcrops of geological formations, tectonic features and other mining-related information. The geophysical data includes total aeromagnetic field data taken on a 1:250,000 scale by the SGM (2000) using a G-B22A optically pumped cesium vapor magnetometer with a sensitivity of 0.01nT. The flight lines were measured on a north-south direction, with a spacing of 1000m and a height above average terrain of 300m. The geomagnetic field in the center of the measured area had an intensity of 47303nT, an inclination of 56o19´ and declination of 7o31´. Initially aeromagnetic data were reduced to the pole using the methodology of both Baranov (1957) and Baranov and Naudy (1964). Once the GIS design had been performed, the qualitative and quantitative interpretation of the aeromagnetic data and their results were also included in the GIS (e.g. magnetic alignments).

The limits of the stratigraphic formations and the location of faults, fold axes and mines were digitized on the geological map, using Didger 3.02 and MapInfo Professional 6.5 software. MapInfo and ArcGIS software were used to assemble and manage the GIS. Information was added to each of the attributes that characterize the objects of the GIS during the assembly process. For example, the object Geology Formation was added information to its attributes, such as names, types of rocks, age, mineralization, etc.

Before beginning the process of managing the GIS, the description and analysis of the magnetic map was performed using Surfer software. A quantitative interpretation of aeromagnetic data using 2D forward modeling was performed during this first stage. This interpretation was carried out along 4 profiles on a north-south direction, thus located in the area in which the main anomalies are found, in order to calculate the depths of the basement and determine any possible subsurface structures. Forward modeling was undertaken using Mag2dc software (Cooper, 2003) which calculates the magnetic field anomalies by means of the Talwani method (Talwani, 1965). This method calculates magnetic anomalies produced by arbitrarily two-dimensional bodies, represented by irregularly shaped polygons in a cross-section. Two groups of rocks were used in the modeling, the first composed by igneous rocks taken from the basement of the basin, with an average magnetic susceptibility of 13x10-3 SI, while the second group includes the sedimentary rocks taken from the basin presented an average magnetic susceptibility of 0 SI. Subsequently, several graphical entities were defined on the magnetic map (contour lines, areas, alignments and points) entities which were exported into the MapInfo and ArcGIS software for inclusion in the GIS database. The entities were then compared with surface geological information to determine their probable relationship with the behavior of the magnetic field. Various thematic maps (e.g. rock types, geological age and tectonics regime) were also generated in the MapInfo and ArcGIS software. These maps were exported to the Surfer software for comparison with the magnetic map.

Two sectors of the study area were selected in order to assess the detail of the geotectonic regime, using the results of the interpretation of the aeromagnetic data. The first sector is located in an area of uplifted blocks in the basement, while the second sector is located inside an area of depressed blocks in the basement.

4. Results and Discussion

4.1. Use of GIS to assess the geotectonic regime using aeromagnetic data reduced to the pole

From the description and analysis of the aeromagnetic data reduced to the pole, positive anomalous zones are shown as elongated mainly on a NW-SE direction (Figure 4). This zone occupies the biggest area of the map (bounded by the contour line with the value 0 nT). As it is considered that the behavior of the magnetic field mainly correspond to the basement rocks of the Sabinas Basin (Pascacio-Toledo, 2001), this area is characterized by uplifted basament blocks (Vázquez et al., 1990; Gunn, 1997) composed of igneous and metamorphic rocks (Pascacio-Toledo, 2001; Jacobo-Albarrán et al., 2011).

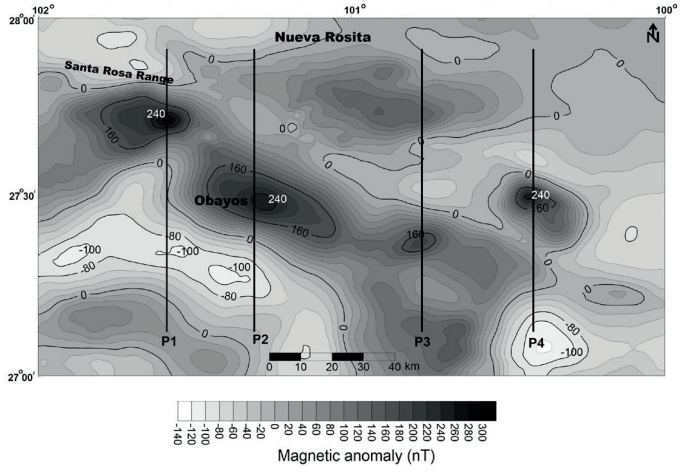

Figure 4. Magnetic anomaly map of Nueva Rosita. Black line indicates the location of 2D profiles (P1, P2, P3 and P4). The magnetic field is expressed in nanotesla (nT).

The 2D models obtained from the 4 profiles show the depths of the basin as varying from 1.5 and 9 km. The deepest zone of the basin is located at the southern end of the P4 profile, while the shallower zone is located in the P2 profile, in the Obayos area. The basement geometry of the basin suggests several faults, which suggest the probable presence of graben and horst. This later structure may be related to the uplifted basement blocks (Figure 5). These results suggest that the 160 nT are contour lines delimit the areas of the basement where the blocks themselves are presumed to be shallower; whereas the contour lines with the value 240 nT indicate the shallower parts of these blocks.

Theoretically, the negative values for the magnetic field should correspond to with the deep zones of the basin (Vázquez et al., 1990), namely the depressed blocks of the basement. Using the 2D models (Figure 5) revealed that the areas with negative values were delimited by isolines of -80 nT, which should define the deepest parts of the basin (Figure 4). Within these areas, the isolines with a value of -100 nT indicate the areas of the basin with the greatest thickness of sedimentary rock, thus indicating that the basement rock is deeper.

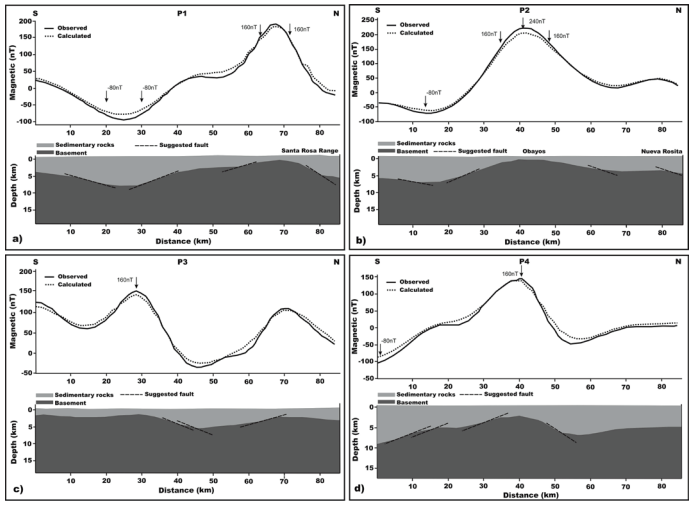

Figure 5. 2D-models of the Sabinas Basin. Arrows indicate the position of the isolines of magnetic field. Location of P1, P2, P3 and P4 are indicated in Figure 4.

The shaded relief map of the aeromagnetic data shows various alignments along the NW-SE and NE-SW trajectories (Figure 6). Most alignments can also be identified in the 2D models (Figure 5), alignments which have been associated with deep faults delimiting the basement blocks (Cruz-Falcón et al., 2010).

Contour lines and magnetic alignments were exported to the GIS and subsequently compared with geological information (e.g., outcrops of different types of rocks, faults and location of mineral deposits). The MapInfo software shows the exported vectors overlapping on the geological map (Figure 3). The comparison of the geological and geophysical information allows the causes for the behavior of the magnetic field to be inferred. The shallower blocks of the basement sometimes cause changes in the sedimentary cover, as seen in the blocks located in the central and NW end of the study region and identified by the letters A and B in Figure 3. Both of these blocks form part of the Obayos anticline and the Santa Rosa Range, with the shape and direction of Block A forming part of the Obayos anticline and following the direction of the fold axis. The NW end of this geological structure is truncated by Block B, which follows a different direction (NE-SW) similar to the Santa Rosa Range.

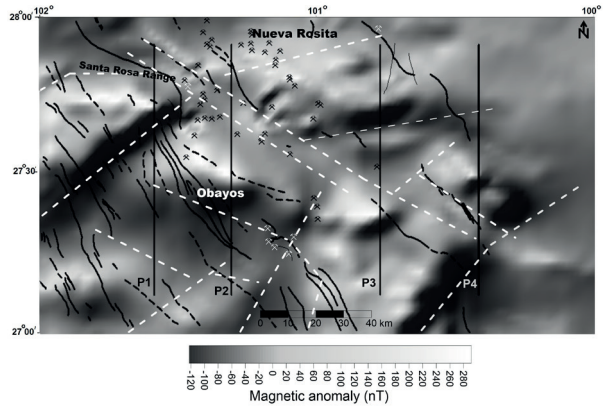

Figure 6. Shaded relief map of the aeromagnetic data for Nueva Rosita. Dashed lines indicate magnetic alignments. Black lines indicate faults and axes of fold (see the legend for Figure 3). Black symbols indicate the location of coal mines and white symbols indicate the location of barite, manganese and Pb-Zn mines. P1, P2, P3 and P4 indicate position of 2D profiles.

The relationship between the characteristics of the magnetic field described here and the geological structures suggest a remobilization of the basement during the Laramide orogeny, in which various deep fault systems were reactivated, thus dividing the basement into blocks. Some of these blocks were uplifted, causing deformations in the sedimentary filling of the basin. The deepest zones of the basin are located south of Obayos and on the SE and NW edges. The areas delimiting these zones and the uplifted blocks of the basement correspond to magnetic alignments. These alignments suggest the probable location of deep fault systems which are likely to be the cause of the geotectonic environment described here. Generally, surface indications of the presence of these faults cannot be found. It is likely that these deep structures affect the sedimentary cover at its lower and medium levels. While these structures could perhaps affect all sedimentary sequences, later surface indications were covered by more recent sedimentary deposits.

The comparison of the magnetic map with the map of rock types shows that the basalts have little influence on the behavior of the magnetic field (Figure 7)as they do not generate a magnetic anomaly due to their very low thickness (an average of approximately 3 meters). These outcrops are located on the edges of uplifted blocks and apparently correspond to faults that follow the alignments of the magnetic field (Figure 3 and 6). Such faults may constitute pathways through which lava spills occurred in this area, volcanic events which occurred during the Pliocene-Pleistocene (Martínez-Rodríguez et al., 2008) and indicate the recent active nature of these presumed faults.

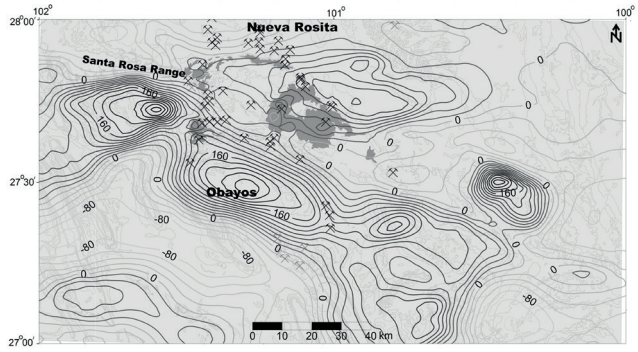

Figure 7. Map of rocks type (sedimentary and igneous rocks) in the Nueva Rosita region. Light gray color represents sedimentary rocks and the dark gray color represents igneous rocks. Lines indicate the contour lines for the magnetic field (black is positive and gray is negative). Black symbols indicate the location of coal mines and gray symbols indicate the location of barite, manganese and Pb-Zn mines.

According to the locations of the main geological structures (folds and faults), the axes of the big anticlines are located on the edges of what appear to be uplifted blocks (Figure 6). Sometimes these axes of folds and small sections of faults correspond to the NW-SE magnetic alignments.

With Figure 6 showing all barite, manganese and Pb-Zn mines as located on the edges of the supposed blocks and apparently corresponding to the faults, the magnetic map shows one important feature of these MVT-Type mineral deposits, namely their proximity to large fault systems (González-Sánchez et al., 2007). Furthermore, most of the coal mines are located on the edges of these blocks or in areas of the basin of intermediate depth. This result demonstrates the effect of the remobilization of the basement on the structural configuration of the region, a remobilization which caused shallow coal seams to be formed.

Comparing the ages of the rock with the magnetic map (Figure 8) reaffirms the relationship between the basement and the tectonic deformations, as most of the areas with high magnetic field values and corresponding to the uplifted blocks of the basement are surrounded by outcrops of Mesozoic rocks, generally very folded and eroded.

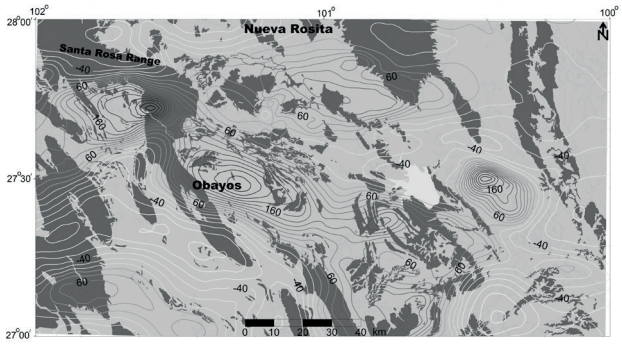

Figure 8. Map of Mesozoic and Cenozoic rocks of the Nueva Rosita region. Dark gray color represents Mesozoic rocks and light gray color represents Cenozoic rocks. Gray and black lines indicate the contour lines for the magnetic field (black is positive and gray is negative).

4.2. Details of the geotectonic regime in two sectors of the Sabinas Basin.

Using the above results, this section presents the details of the geotectonic regime in two sectors of the Sabinas Basin, sectors referred to hereafter as Example 1 and Example 2 (Figure 9). Detailed analysis was undertaken in these sectors to confirm the results of the interpretation of the aeromagnetic data, which suggested uplifted and depressed basement blocks. The following analytical steps and results are described below.

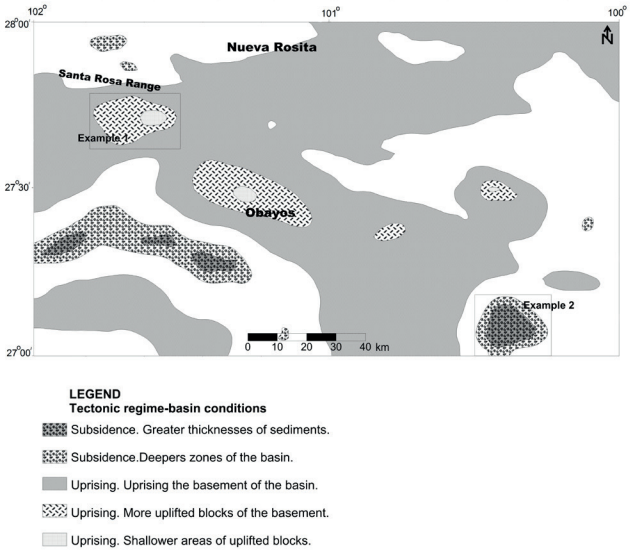

Figure 9. Geotectonic regime map of the Sabinas Basin. Rectangles delimit the zones for examples 1 and 2.

4.2.1. Management of databases

Initially the magnetic field data were interpolated to create a map in raster format, which was classified into five classes of relevance taking into account the different ranges of the magnetic map indicate by the contour lines in Figure 4. These contour lines delineate the areas with different levels of the tectonic regime of the basin. The map depicts each of the classes and the different attributes of the tectonic regime, as well as the corresponding effect on the basin (Table 1). Classes 1 and 2 present negative values for the magnetic field and include the zones of the basin in which predominates the tectonic regime of subsidence, which is recorded at great depths, mainly in the zones of corresponding to Class 1. The zones presenting an uprising tectonic regime are indicated in three classes, with positive values for the magnetic field that indicate a different order of uprising for the basement blocks.

Table 1. Classes of the magnetic field map.

Classes	Magnetic field values (nT)	Attribute of tectonic regime	Response in the basin
1	≤-100	Subsidence	Deeper zones of the basin (larger thick sediments)
2	- 99 a -80	Subsidence	Deep zones of the basin
3	0 a 159	Uprising	Uprising the basement of the basin
4	160 a 239	Uprising	More uplifted blocks of the basement
5	≥240	Uprising	Shallower areas of uplifted blocks

The characteristics of some of these areas are detailed in the two examples shown below.

4.2.2. Example 1.

The geotectonic regime map in the Sabinas Basin (Figure 10) indicate that the sector represented by Example 1 is located within a positive magnetic field anomaly (Figures 3 and 9) representing one of the sectors of more uplifted blocks of the basement in the basin. In the inside of this sector is also delimited the shallower area of the block. The spatial analysis results for the shallower area of the uplifted block in this sector are shown in Table 2. The combination of geotectonic regime map with the geological map indicates that in this area predominate Cretaceous rocks on the surface (Figure 10), with mainly Late Cretaceous covering more than 69% of the area (Table 2). This indicates uplift and the erosion of the youngest geological formations, according to the results of other studies (Buccolini et al., 2014; Wu et al., 2014). This uprising regimen is corroborated by the presence of Holocene colluvial sediments formed by piedmont deposits covering 27% of the area, with the few alluvial deposits identified in the area revealing a sector of uprising, where erosion processes predominate compared to cumulative processes. This approach is validated by other research results (Shikakura, 2012; Medvedev and Harst, 2015).

Table 2. Spatial distribution of the shallower area of uplifted blocks in the sector for Example 1.

Age	Type of rocks and sediments	Area (km²)	% of area
Cenozoic	Colluvium	10.66	27.04
	Alluvium	0.43	1.09
Late Cretaceous	Sedimentary	27.44	69.64
Early Cretaceous	Sedimentary	0.88	2.23

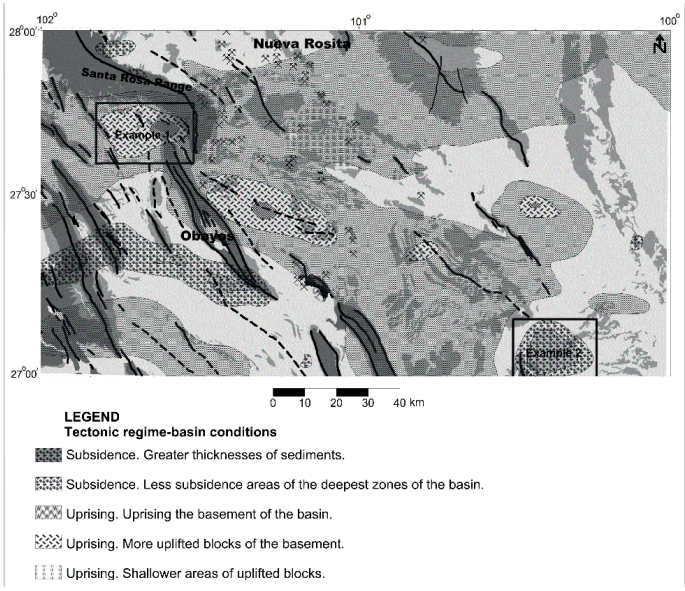

Figure 10. Combination of geotectonic regime map with the geological map in the Sabinas Basin. The legend of the geological map is shown in Figure 3. Rectangles delimit the zones for examples 1 and 2.

4.2.3. Example 2.

The sector illustrated by Example 2 is located in a negative anomaly of the magnetic field (Figures 3 and 9), associated with zones of subsidence of the basin. In this sector the magnetic field values below of -100 nT delimit the deeper area of the sector, i.e. larger thick sediments. Table 3 shows the results of the spatial analysis conducted on the deeper area found within the sector. According to the combination of geotectonic regime map with the geological map it is noted that 91 % of the area is covered by Holocene deposits, i.e., alluvium, colluvium and conglomerates, as well as a small area of Cretaceous rock (Figure 10). These attribute indicate a regime of tectonic stability with a prevalence of cumulative erosion processes (Shikakura, 2012; Medvedev and Harst, 2015).

Table 3. Spatial distribution of the area with greater thicknesses of sediments in the sector for Example 2.

Age	Type of rocks and sediments	Area (km^2)	% of area
Cenozoic	Alluvium	80.43	48.15
	Colluvium	9.00	5.39
	Conglomerates	62.63	37.49
Late Cretaceous	Sedimentary	14.99	8.97

5. Conclusions

The analysis carried out in this study highlights the importance of the use of GIS for the interpretation of geophysical data, particularly data pertaining to the total magnetic field as used to characterize the geotectonic regime of a basin. The interpretation of the magnetic data was carried out both qualitatively and quantitatively, with the latter interpretation made using 2D models. The results of this study enabled the following: an analysis of the magnetic field; the generation of graphical entities; the definition of areas with certain geological significance, such as areas thought to correspond to the uplifted blocks of the basement in the Sabinas Basin and its deeper areas; and, the identification of the alignment of the magnetic field that probably correspond to fault systems. The nature of the magnetic anomalies was assessed by comparing these graphical entities with geological information by means of GIS. A remobilization of the basement in the Sabinas Basin during the Laramide orogeny is evidenced from the relationship between the magnetic field and the geological structures. This relationship suggests that, during the orogeny, various deep fault systems were reactivated, thus dividing the basement into blocks which were uplifted, causing deformations in the sedimentary filling of the basin. The development of thematic maps using GIS, such as maps drawn based on rock type, age and tectonics, enables an accurate and precise comparison with the aeromagnetic data. The main structural deformations observed on the surface, as well as the principal areas with mineral deposits and lava spills, correspond to the edges of the presumed uplifted blocks of the basement. The results enabled researchers to detail the geotectonic regime in two sectors within the study area, which are linked to uprisings and subsidence in the basin. A prevalence of erosion processes were identified in the sector where uprisings were recorded in the basin whereas the cumulative processes predominate in the sector showing subsidence. The analysis conducted here on the tectonic regime in two sectors supports the concept pertaining to the dynamics identified in the basement blocks, which indicated uplifted and depressed blocks, suggested by the interpretation of the aeromagnetic data.

Acknowledgements

We thank to the Autonomous University of Coahuila for the support it has provided for this research.

References

Baranov, V. (1957). A new method for interpretation of aeromagnetic maps, pseudogravimetric anomalies, *Geophysics*. 22, 359-383.

Baranov, V. and Naudy, H. (1964). Numerical calculation of the formula of reduction to the magnetic pole, *Geophysics*. 29, 67-79.

Buccolini, M., Materazzi, M., Aringoli, D., Gentili, B., Pambianchi, G. and Scarciglia, F. (2014). Late Quaternary catchment evolution and erosion rates in the Tyrrhenian side of central Italy, *Geomorphology*. 204, 21-30.

Chávez-Cabello, G., Aranda-Gómez, J.J. y Iriondo-Perrone, A. (2011). Culminación de la Orogenia Laramide en la Cuenca de Sabinas, Coahuila, México, *Boletín de la Asociación Mexicana de Geólogos Petroleros*, A.C. 56, no. 1-2, 80-91.

Chávez-Cabello, G., Aranda-Gómez, J.J., Molina-Garza, R.S., Cossío-Torres, T., Arvizu-Gutiérrez, I.R. and González-Naranjo, G.A. (2005). La falla San Marcos: una estructura jurásica de basamento multirreactivada del noreste de México, *Boletín de la Sociedad Geológica Mexicana*. **57**, 27-52.

Cooper G.R.J. (2003). Mag2dc 2.10. An interactive 2.5D Magnetic modelling and inversion program for Microsoft windows, School of Geosciences University of the Witwatersrand, Johannesburg 2050 South Africa.

Corona-Esquivel, R., Tritilla, J., Benavides, M.E., Piedad-Sanchez, N. and Ferrusquía, I. (2006). Geología, estructura y composición de los principales yacimientos de carbón mineral en México, *Boletín de la Sociedad Geológica Mexicana*. 57, no. 4, 141-160.

Cruz-Falcón, A., Vázquez-González, R., Ramírez-Hernández, J., Salinas-González, F., Nava-Sánchez and Troyo-Diéguez, E. (2010). Depth estimation to crystalline basement in the valley of La Paz, Baja California Sur, Mexico, *Geofísica Internacional*. 49, no. 4, 213-224.

Eguiluz de Antuñano, S. (2001). Geologic Evolution and Gas Resources of the Sabinas Basin in Northeastern Mexico. In C. Bartolini, R.T. Buffler & A. Cantú-Chapa (Eds.), The western Gulf of Mexico Basin: Tectonics, sedimentary basins, and petroleum systems, *AAPG Memoir*. **75**, 241-270.

González-Sánchez, F., González-Partida, E., Canet, C., Atudorei, V., Alfonso, P., Morales-Puente, P., Cienfuegos-Alvarado, E. and González-Ruiz, L. (2015). Geological setting and genesis of stratabound barite deposits at Múzquiz, Coahuila in northeastern Mexico, Ore Geology Reviews. doi:10.1016/j.oregeorev.2015.10.008

González-Sánchez, F., Puente-Solís, R., González-Partida, E. y Camprubí, A. (2007). Estratigrafía del Noreste de México y su relación con los yacimientos estratoligados de fluorita, barita, celestina y Zn-Pb, *Boletín de la Sociedad Geológica Mexicana*. **59**, no. 1, 43-62.

Gunn, P.J. (1997). Application of aeromagnetic surveys to sedimentary basin studies, AGS*O Journal of Australian Geology & Geophysics*. **17**, no. 2, 133-144.

Jacobo-Albarrán, J., González-Pineda, J.F., Muñoz-Cisneros, R. y Rosales-Rodríguez, J. (2011). Actualización petrológica del basamento cristalino de la Cuenca de Sabinas, *Boletín de la Asociación Mexicana de Geólogos Petroleros, A.C.* **56**, no. 1-2, 105-112.

Khemiri, S., Mansouri, S., Khnissi, A. and Zargouni, F. (2013). Implementation of GIS and Geographic RDBMS Prototype for Water Resources Management. Zeuss-Koutine Basin, *Journal of Geographic Information System*. **5**, 429-445.

Martínez-Rodríguez, L., Miranda, A., Pérez, M.A., Romero, I. y Sánchez, E. (2008). Carta geológico-minera Nueva Rosita G14-1, Coahuila y Nuevo León, 1:250000, *Servicio Geológico Mexicano*. 1 mapa.

Medvedev, S. and Hartz, E.H. (2015). Evolution of topography of post-Devonian Scandinavia: Effects and rates of erosion, *Geomorphology*. **231**, 229-245.

Pascacio-Toledo, R. (2001). Texto guía Carta magnética de Nueva Rosita G14-1, 1:250000, *Consejo de Recursos Minerales*. 19 p.

SGM (2000). Carta magnética de campo total Nueva Rosita G14-1, Estado de Coahuila, 1:250000. *Servicio Geológico Mexicano*.

Shikakura, Y., Fukahata, Y. and Matsu'ura, M. (2012). Spatial relationship between topography and rock uplift patterns in asymmetric mountain ranges based on a stream erosion model, *Geomorphology*. **138**, no. 1, 162-170.

Talwani, M. (1965). Computation with the help of a digital computers of magnetic anomalies caused by bodies of arbitrary shape, *Geophysics*, **30**, 797-817.

Telford, W.M., Geldart, L.P. and Sheriff, R.E. (1990). *Applied geophysics,* Second edition: Cambridge University Press, 770 pp.

Vázquez, A.A., Ruiz, R.J. y González-Morán, T. (1990). Exploración del basamento en el SW de San Luis Potosí, México, utilizando datos gravimétricos, aeromagnéticos y sondeos magnetotelúricos, *Geofísica Internacional*. **29**, no. 2, 71-88.

Wu, L., Xiao, A. and Yang, S. (2014). Impact of wind erosion on detecting active tectonics from geomorphic indexes in extremely arid areas: a case study from the Hero Range, Qaidam Basin, NW China, *Geomorphology*. **224**, no. 1, 39-54.

Ziaii, M., Abedi, A., Ziaei, M., Kamkar-Rouhani, A. and Zendahdel, A. (2010). GIS modelling for Au-Pb-Zn potential mapping in Torud-Chah Shirin area- Iran, *International Journal of Mining & Environmental Issues*. **1**, no. 1, 17-27.